Stability of Fast Solitary Structures on Auroral Field Lines

Ilan Roth and Laurent Muschietti

Space Sciences Laboratory
University of California
Berkeley, CA 94720

Manuscript submitted to

Physics and Chemistry of the Earth

November 16 1999

Abstract

The stability of the fast solitary structures which were observed onboard several auroral crossing satellites is analyzed as a dynamical system and investigated numerically. These large-amplitude potential spikes are supported by trapped electron populations. For parameters of low and mid-altitude auroral passes with gyro-to-bounce frequency ratios significantly larger than unity, the potential spikes are very resilient, while for lower magnetic fields, at ratios below unity, they develop unstable undulations in the transverse direction. The evolution of the solitary structures is related to changes in the trajectories of the trapped electrons. It is shown here that the coupling of the parallel and perpendicular dynamics is stronger when the above ratio decreases, resulting in a bifurcation of trajectories. The addition of a small perturbation to the large amplitude structure leads to a very different response of the trapped electrons in the two configurations. The electron behavior reflects the lack of spike stability at small gyro-to-bounce frequency ratios.

1 Introduction

One of the recent most interesting magnetospheric discoveries is the observation of solitary structures which move rapidly along auroral magnetic field lines. Specifically, with the improved (burst mode) time resolution in measuring electromagnetic fields afforded by the Polar satellite (8×10^3 samples/sec) and the Fast satellite (2×10^6 samples/sec), it became possible to simultaneously get detailed profiles of the potential spikes (Ergun et al., 1998) as well as reasonably good distribution functions of the electrons (Carlson et al., 1998). The most interesting of the newly observed spikes generally move in the anti-Earth direction with a velocity on the order of the electron velocity spread, much higher than ion velocities. These localized, large-amplitude structures are supported by inhomogeneous, non-thermal, trapped electron populations, while they modulate the trajectories of the passing electrons. The evolution and stability of the spikes depends on the adjustment of the trapped population to perturbations and to externally changing parameters.

Generally, the description of an electromagnetic interaction in plasma physics is based on the conservation of phase-space density in the absence of external sinks/sources and Coulomb losses. In this (Vlasov) description the particles are moving along their characteristics, i.e. trajectories in phase space influenced by electromagnetic fields, while self-consistently modifying these fields. In the standard theoretical development, to deal with the inherent nonlinearity of the interaction, one linearizes the equations and finds the eigenmodes for small wave perturbations. The approximation of small-amplitude deviations from a homogeneous equilibrium neglects higher-order terms in the perturbed expansion and this neglect is partly compensated by the lack of stationarity in the solutions, i.e. instability. Experimentally, this description is equivalent to a presentation of the slowly changing wave features by power spectra obtained from a Fourier transform of the electric fields. On the other hand, instead of linearizing the basic equations, one might, from the very beginning, look for a nonlinear description of the interaction by invoking self-consistent, propagating, localized structures of finite amplitude that are supported by a particular distribution function. The self-consistency is assured by constructing the distribution function with the help of constants of motion that are solutions of the characteristic equations. The very fact that the improved observations record numerous localized spikes which propagate over long distances along the geomagnetic field lines indicates that the nonlinear localized pulses can often describe the results of a self-consistent interaction in magnetized plasmas via the (nonlinear) mathematical functional dependence of waveforms. Although Fourier spectra of a collection of spikes can be similar to the linear description, their interaction and the subsequent evolution of the system may be very different.

In this paper we discuss the stability of the nonlinear pulses from the viewpoint of the dynamics of the electrons that support them. We show how variations in plasma parameters affect the dynamics of the trapped electrons and cause the localized spikes to undulate in the transverse direction and destabilise in changing external circumstances.

2 The structure of the trapped electrons

The observations of spikes moving along field lines with varying amplitudes, widths and speeds indicate that they are stable and resilient to perturbations over a broad range of parameters. The spikes are electrostatic (in their frame) and are observed over broad ranges of altitudes, plasma densities and magnetic fields (Ergun et al., 1998; Cattell et al., 1999). Since they pass the satellite with high speed and the time needed to accumulate data for the electron population is generally longer than the transit time of the pulse, we are limited to only partial information regarding the distribution function. Using the available distribution functions and the best fit for the measured spikes, a self-consistent analysis of the trapped distribution which supports a Gaussian pulse with a flat-top population of passing electrons was constructed (Muschietti et al., 1999). The stability boundary for that distribution showed that amplitude and width grow together, indicating that the nonlinear structure is different from a standard soliton or ion hole, and may be considered as an electron hole. The experimental values of the amplitude vs width relation for a large number of spikes was shown to satisfy well this stability boundary (Muschietti et al., 1999). In the self-consistent particle-in-cell simulations, an electron performs gyration around the constant magnetic field with frequency Ω and bounce motion in the potential field with frequency ω_b. The simulations showed that the spikes are very robust and resilient (as they move with high velocity with respect to the ions) when the gyro-to-bounce frequency ratio satisfies $\Omega/\omega_b > 1$, and are destabilized at lower ratios.

3 The dynamics of the trapped electrons

In this section we discuss the trajectories of the trapped, magnetized electrons in the presence of one or two-dimensional potential forms. The self-consistent simulations employ millions of particles making it difficult to analyze their phase space dynamics directly; hence, we impose given fields as observed in the full particle simulations, and follow representative electrons in phase space to discern the changes in their orbits under different external conditions.

We move to the frame of the spike and calculate the trajectories of the electrons and observe the changes in the dynamics of the particles. Following the configuration of the simulations, the electrostatic potential is chosen as

$$\phi(z,x) = \psi_o \; \eta(z,x) \; = \psi_o \; exp \; (-z^2/2\delta_{||}^2) \; exp \; (-x^2/2\delta_{\perp}^2) \tag{1}$$

where z (x) is the parallel (perpendicular) coordinate with respect to the external magnetic field, $\delta_{||,\perp}$ denote the appropriate scale lengths, ψ_o is the amplitude and $\eta(z,x)$ is the Gaussian potential form factor.

In this given potential (to be completed later with additional terms) and external magnetic field we propagate in time (for each particle) a six-dimensional phase space vector $\mathbf{X} = (x, y, z, v_x, v_y, v_z)$. The set of coupled equations

$$\dot{\mathbf{X}} = \mathbf{G}(\mathbf{X}) \, , \tag{2}$$

where $\mathbf{G}$ propagates the particle via the prescribed electromagnetic fields (external constant magnetic field and electric field derived from Eq. (1)), is solved with an adaptive time step. The results are displayed as time series or two-dimensional projections of the phase diagram. Due to the structure of the electromagnetic forces, Eq. (2) describes an autonomous (no time dependence on the RHS) and conservative (volume preserving, i.e. $\nabla \cdot \mathbf{G} = 0$) system.

In Figure 1 we show the time series oscillations of the parallel (a) position, (b) velocity, and (c) energy of a low-energy electron in the presence of a one-dimensional Gaussian potential ($\delta_{\perp} >> \delta_{||}$). Since effectively the potential has only parallel dependence, the phase space dynamics is two-dimensional (one degree of freedom) and, for this low kinetic energy, the motion of the electron is equivalent to a linear harmonic oscillator. Figure 1d shows the phase space (z, v_z) of this electron. Similarly to a standard linear pendulum, the low-energy electron performs sinusoidal motion in the time series plots and a circular motion in phase space. The normalized oscillation, or bounce frequency is given by $\omega_b = [\psi_0/\delta_{||}^2]^{1/2}$.

Figures 2a-c show similar time series oscillations for a more energetic electron in the vicinity of the separatrix, while Figure 2d depicts the trajectories in the truncated phase space for ten different electrons, equally spaced in their initial parallel velocity. One observes the big increase in the period as the particles approach the separatrix, the deformation from the sinusoidal behavior of Figure 1 and from a circle in phase space, typical of a nonlinear pendulum.

We now turn to the phase space trajectories for a two-dimensional potential with a finite perpendicular electric field ($\delta_\perp/\delta_{||} = 2$). The magnetic field is weak, such that $\Omega/\omega_b < 1$. Figures 3a-c show cuts in the contracted phase space for a single particle, while the projected phase space for ten particles with increasing parallel velocity is shown in Figure 3d. One observes that the coupling between parallel and perpendicular dynamics emphasizes a small irregularity in phase space dynamics and that, with kinetic energy increasing, the electron phase space gets smeared with respect to the previously regular harmonic motion. An electron performs bounce motion and gyration simultaneously and as it crosses magnetic field lines, the electric field changes along its trajectory. Particles which encounter the largest changes of this field are affected mostly, so that the distribution function of the electrons which support the spike is modified. We also note that the gyroradius is changing along the trajectory (Fig 3a). The dynamics will be now enriched by the addition of a small perturbation to the potential of Eq. 1.

4 Modification in the dynamics due to imposed perturbation

Particle-in-cell simulations indicate that the one or two-dimensional spikes are very robust for strong magnetic field (Muschietti et al., 1999); however, while lowering the magnetic field (gyro-to-bounce frequency < 1), one observes a growing, transverse undulation in the potential contours, which eventually results in a collapse of the spike.

Accordingly, we add the following potential term to Eq. 1

$$\delta\phi_1(z, x) = \psi_1 \; (z/\delta_{||}) \; \eta(z, x) \; sin(kx) \tag{3}$$

where $\psi_1 \; << \psi_o$ and k denotes the perpendicular wavenumber of the perturbation with

$k\rho < 1$. Eq. 3 introduces a small amplitude perturbation with long wavelength as observed in the self-consistent simulations.

In the same format as Figure 3, Figure 4 shows results with the additional potential of Eq. 3. The amplitude of the perturbation is $\psi_1/\psi_0 = 0.08$ and its wavenumber satisfies $k\rho = 0.4$. One observes large deviations in the perpendicular phase space cuts and merging of trajectories in the parallel phase space. This strong irregularity in the phase space indicates a lack of sustainability of the distribution that supports the nonlinear spike. If we now increase the gyro-to-bounce ratio, we do not observe these large phase space deformations (corresponding figure not shown).

5 Summary

Localized potential spikes, as observed onboard auroral satellites, are supported by inhomogeneous electron distribution functions that depend on the constants of motion. We have described the changes which occur in particle trajectories when the electrons are subjected to externally changing conditions. We showed that the regular motion in a one-dimensional Gaussian potential exhibits typical pendulum dynamics; the low-energy particles follow linear oscillations, while the electrons close to the separatrix follow the nonlinear oscillatory pattern. For gyro-to-bounce frequency ratios smaller than unity and in the presence of a two-dimensional Gaussian potential, which creates an inhomogeneous perpendicular field, we observe a start of bifurcation with a smearing of phase space. This allows small close encounters between trajectories that belong to different initial energies. No such effect is observed at larger gyro-to-bounce ratios. The addition of a small perturbation enhances the effect significantly. Since large distortions in phase space modify the distribution function that supports the spike, we expect the spike to lose its stability whenever the gyro-to-bounce frequency ratio becomes small ($\Omega/\omega_b < 1$).

Acknowledgements. The authors acknowledge fruitful discussions with C. Carlson, R. Ergun, F. Mozer, and C. Cattell. This work was supported by NASA grants NAG5-6985, NAG5-3596, and NAG5-3182.

References

Ergun et al, *Geoph. Res Lett* , **25**, 2041, 1998.

Carlson et al, *Geoph. Res Lett* , **25**, 2017, 1998.

Cattell et al, *Geoph. Res Lett* , **26**, 425, 1999.

Muschietti et al, *Geoph. Res Lett* , **26**, 1093, 1999; **26**, 1689, 1999.

Figure Captions

Fig. 1. Time series and phase space of a low-energy electron in an effectively one-dimensional Gaussian potential structure. (a) position, (b) velocity, (c) total energy vs time; (d) v_z vs z. The position is normalized to the initial gyroradius ρ, the velocity to the thermal spread, the potential to the temperature and the time to the inverse gyrofrequency Ω^{-1}. Gyro-to-bounce frequency ratio is $\Omega/\omega_b = 3.0$, parallel scale length is $\delta_{||}/\rho = 2$, aspect ratio is $\delta_\perp/\delta_{||} = 100$ and the ratio of kinetic to potential energy is 6×10^{-3} .

Fig. 2. Time series similarly to Figure 1a-c, for an electron close to the separatrix (ratio of kinetic to potential energy is 0.95) and (d) phase space for 10 electrons with equidistant parallel velocities in a one-dimensional potential structure.

Fig. 3. Truncated phase space cuts (a-c) for a single electron and parallel phase space (d) for 10 electrons with equidistant parallel velocities in a two-dimensional potential structure. Parameters: $\delta_\perp/\delta_{||} = 2$, $\delta_{||}/\rho = 2$, and $\Omega/\omega_b = 0.6$. Initial and final values are denoted by 'in' and 'f', respectively.

Fig. 4. Truncated phase space cuts (a-c) for a single electron and parallel phase space (d) for 10 electrons with equidistant parallel velocities. The potential structure is the two-dimensional structure of Fig 3 modified with the perturbation $\delta\phi_1$ (see Eq. 3). Parameters: $\psi_1/\psi_o = 0.08$, $k\rho = 0.4$, and $\Omega/\omega_b = 0.6$.

Figures

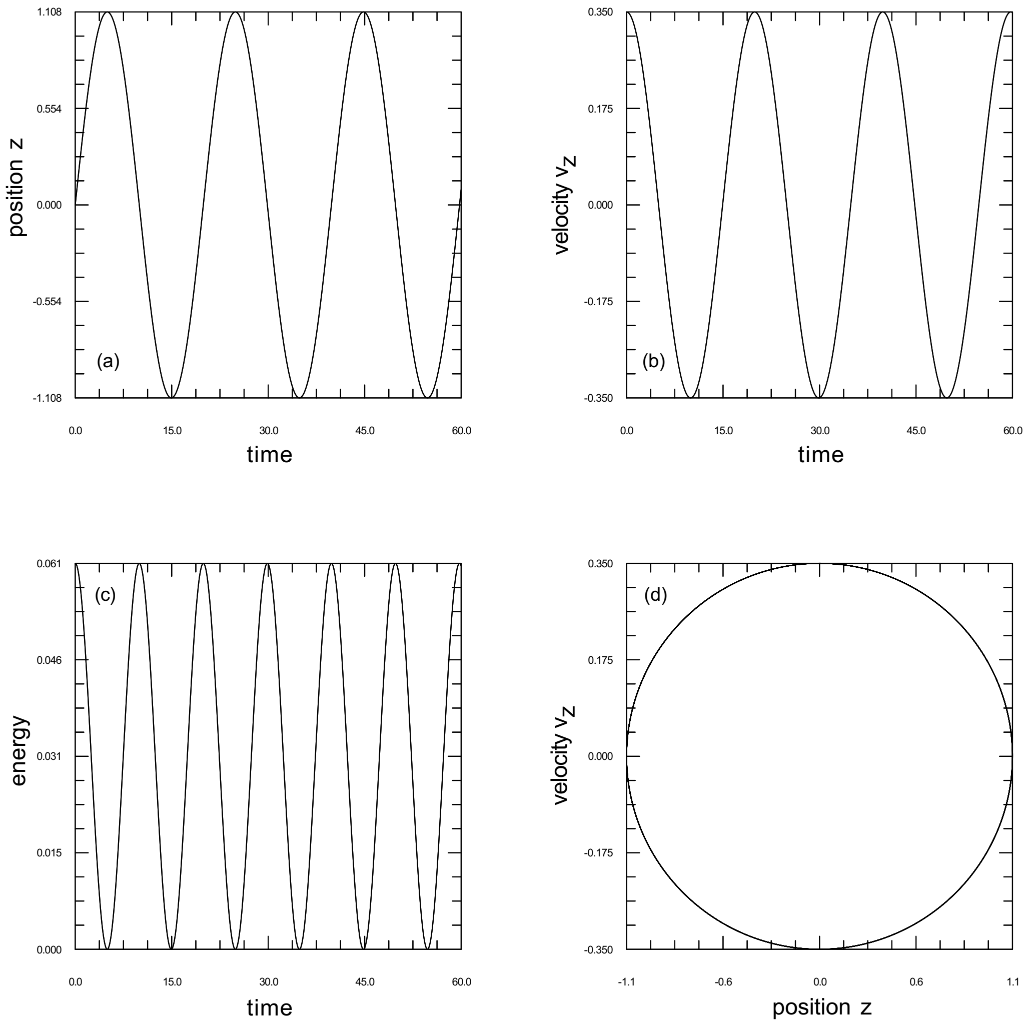

Fig. 1. Time series and phase space of a low-energy electron in an effectively one-dimensional Gaussian potential structure. (a) position, (b) velocity, (c) total energy vs time; (d) v_z vs z. The position is normalized to the initial gyroradius ρ, the velocity to the thermal spread, the potential to the temperature and the time to the inverse gyrofrequency Ω^{-1}. Gyro-to-bounce frequency ratio is $\Omega/\omega_b = 3.0$, parallel scale length is $\delta_{||}/\rho = 2$, aspect ratio is $\delta_{\perp}/\delta_{||} = 100$ and the ratio of kinetic to potential energy is 6×10^{-3} .

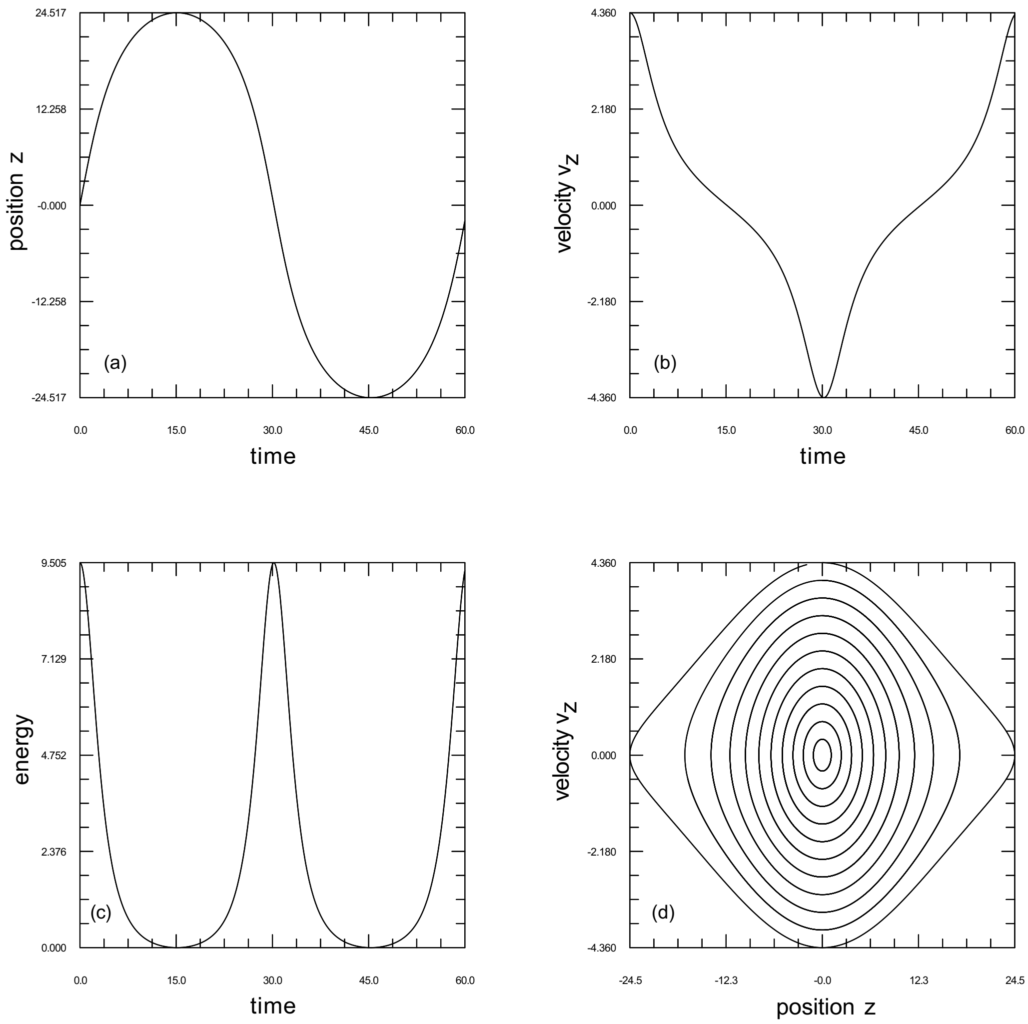

Fig. 2. Time series similarly to Figure 1a-c, for an electron close to the separatrix (ratio of kinetic to potential energy is 0.95) and (d) phase space for 10 electrons with equidistant parallel velocities in a one-dimensional potential structure.

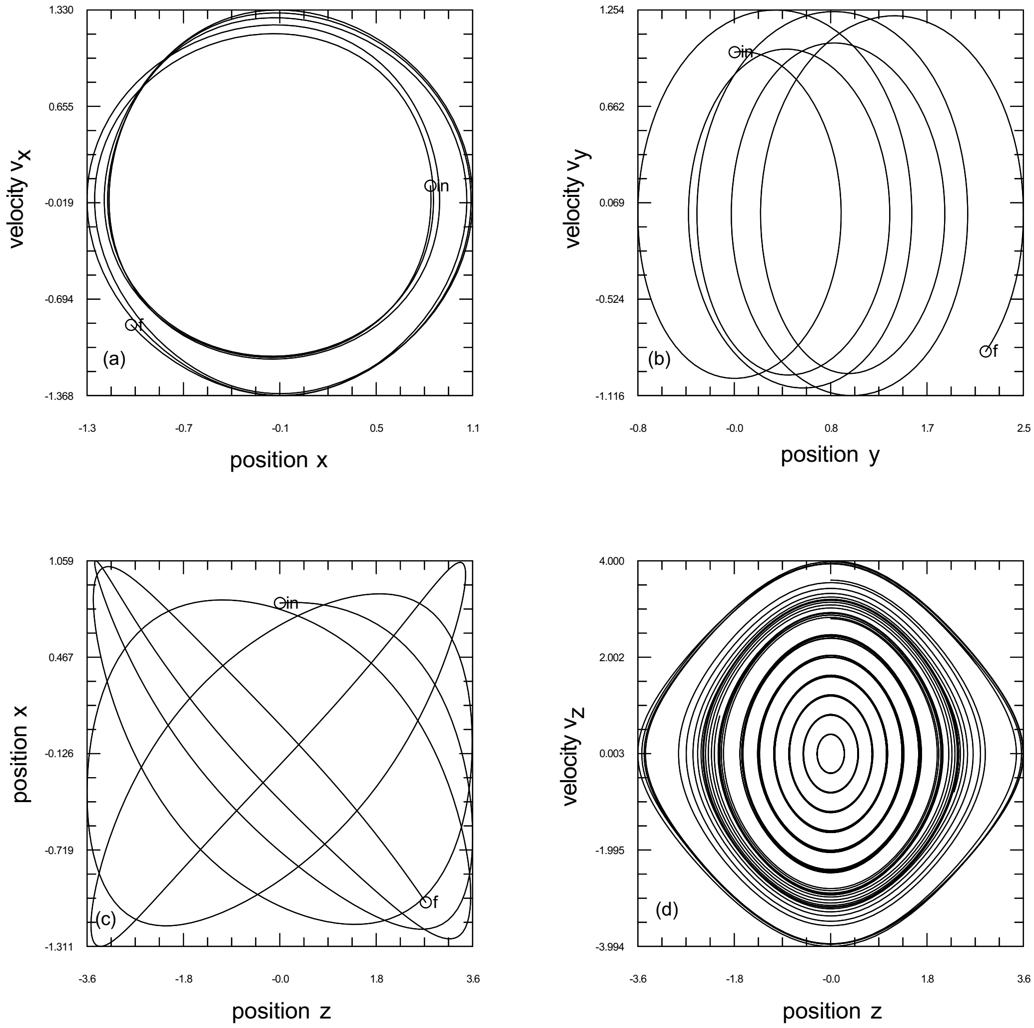

Fig. 3. Truncated phase space cuts (a-c) for a single electron and parallel phase space (d) for 10 electrons with equidistant parallel velocities in a two-dimensional potential structure. Parameters: $\delta_\perp/\delta_{||} = 2$, $\delta_{||}/\rho = 2$, and $\Omega/\omega_b = 0.6$. Initial and final values are denoted by 'in' and 'f', respectively.

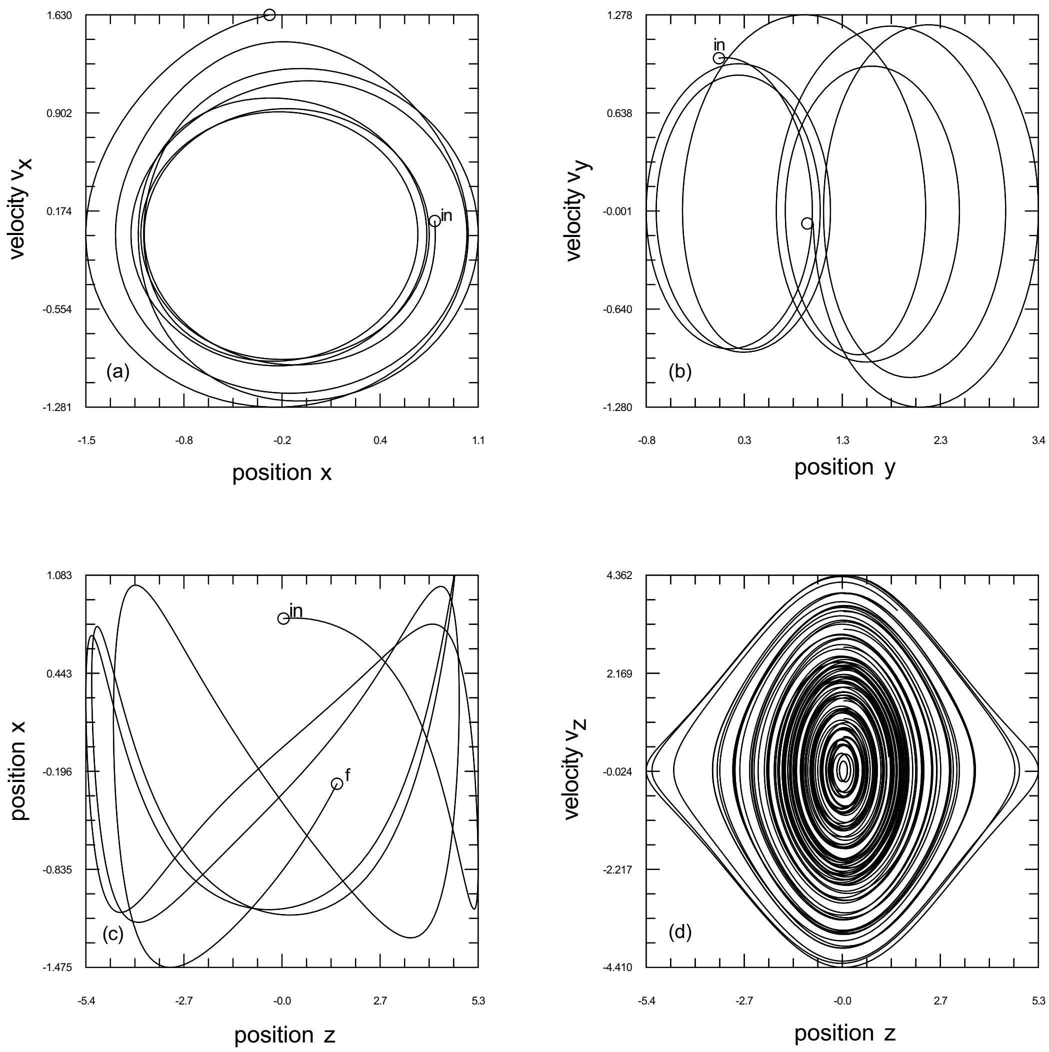

Fig. 4. Truncated phase space cuts (a-c) for a single electron and parallel phase space (d) for 10 electrons with equidistant parallel velocities. The potential structure is the two-dimensional structure of Fig 3 modified with the perturbation $\delta\phi_1$ (see Eq. 3). Parameters: $\psi_1/\psi_o = 0.08$, $k\rho = 0.4$, and $\Omega/\omega_b = 0.6$.